

## Hydrothermally Synthesized NanoTiO<sub>2</sub> Thick Films for Gas Sensing Application

GANESH J. MOGAL<sup>1</sup>, DAGA V. AHIRE<sup>1</sup>, G. E. PATIL<sup>2</sup>,  
F.I. EZEMA<sup>3</sup> and GOTAN H. JAIN<sup>2\*</sup>

<sup>1</sup>Materials Research Lab, K.T.H.M. College, Nasik 422013 India

<sup>2</sup>Department of Physics, SNJBs K.K.H.A. Arts, S.M.G.G.L. Commerce and Science College, Chandwad 423101 India

<sup>3</sup>Department of Physics & Astronomy, University of Nigeria, Nsukka, Enugu State, Nigeria  
*gotanjain@rediffmail.com*

Received 3 November 2014 / Accepted 28 November 2014

**Abstract:** TiO<sub>2</sub> nanoparticles were prepared by hydrothermal synthesis technique. The thick films of TiO<sub>2</sub> were prepared by screen printing technique; gas sensing performance of this film was tested for various gases. The film showed highest response and selectivity to H<sub>2</sub>S gas. The gas response selectivity of film were measured and presented. The films were characterized by x-ray diffraction (XRD), Scanning Electron Microscopy (SEM), Transmission Electron Microscopy (TEM), Selected Area diffraction and optical absorption spectroscopy technique. The quick response and fast recovery are the main features of these films. The effect of temperature on the optical, structural, morphological and gas sensing properties of the films were studied and discussed.

**Keywords:** TiO<sub>2</sub>, Hydrothermal synthesis, Thick films, Gas sensor, Screen-printing technique

### Introduction

Accompanying the acceleration of urbanization and industrialization, air pollution has become one of the most serious environmental problems on earth. It affects not only human health but also the health of ecological system. The atmosphere protects life on earth by absorbing ultraviolet solar radiation, warming the surface through heat retention, and reducing temperature extremes between day and night. However, severe loss of stratospheric ozone has been detected in the high latitudes of the Northern Hemisphere as well as over the Antarctic. At the same time, intensification of ultraviolet radiation has been observed. Ultraviolet radiation is known to a danger to human beings as well as having an effect on agricultural, forests and water ecosystems.

Global air pollution studies have been an important topic. The observation and collection of reliable data on regional and global air quality has a rather brief history. Routine atmospheric measurements of gas and particle concentrations have been conducted at sites with ground based instruments.

Other amenities such as home appliances and security systems in combination with advanced electronics also utilize sensors to give outstanding performance. Similarly, sensors have been extensively used in the medical field for diagnostic and therapeutic purposes and also for environmental monitoring of pollution hazards. With the growing awareness of the harmful effects of industrial wastes, emissions from vehicles exhausts, *etc.*, various types of sensors are necessary as pre-requisites to detect these toxic pollutants before converting them into harmless products.

In the recent research sensors have attracted a great deal of attention from scientists and engineers. Even in the near future, it is expected to gain important in view of the construction of more or less intelligent ensembles, which integrate actuating, sensing and computing subsystems. Detection of various gases using solid state chemistry has generated a great deal of interest, both in academia and in industry.

The catalytic, electronic and optical properties of TiO<sub>2</sub> made it an important material for application such as dye sensitized solar cell<sup>1,2</sup>, sensor<sup>3</sup>, photocatalysis<sup>4,5</sup> and photo splitting of water<sup>6</sup>. The electronic properties depend on their atomic structure and shape of TiO<sub>2</sub>.

## Experimental

The TiO<sub>2</sub> nanoparticles were synthesized by a hydrothermal process and using commercial Ti(IV) isopropoxide powder (98% from Acros Organics) as source material. In detail, 3.6 g of Ti isopropoxide powder was mixed with 100 mL of water and stirred at room temperature. Isopropoxide immediately hydrolyzed, forming an amorphous precipitate. The suspension was repeatedly centrifuged, filtered and washed with distilled water. Finally, after last filtration, 160 mL of distilled water was added for hydrothermal experiments. The mixture was put into a Teflon-lined stainless autoclave which was heated at 180 °C for 12 h, after that it was naturally cooled down to room temperature. The obtained precipitation was filtered and washed in deionized water.

The thixotropic paste<sup>7-10</sup> was formulated by mixing the fine synthesized power of TiO<sub>2</sub> with solution of ethyl cellulose (as temporary binder) and organic solvents. The paste was screen printed on glass substrate in desired patterns; the prepared films were fired at 550 °C for 30 min.

The sensing performance of the thick films was examined by using a static gas sensing system<sup>11,12</sup>. To heat the sample up to required operating temperatures, the heater was fixed on the base plate. A thermocouple is connected to a digital temperature indicator for temperature measurement. The required gas concentration inside the static system was achieved by injecting a known volume of test gas using a gas-injecting syringe.

## Results and Discussion

### *Microstructural analysis by using SEM*

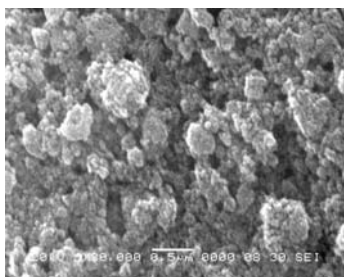
The micro structural and chemical compositions of the films were analyzed using a scanning electron microscope (SEM, JEOL JED 6300) coupled with an energy dispersive spectrometer (EDS, JEOL JED 2300LA).

Figure 1 depicts a SEM image of TiO<sub>2</sub> thick film fired at 550 °C. The film consists of voids and a wide range of particles distributed uniformly.

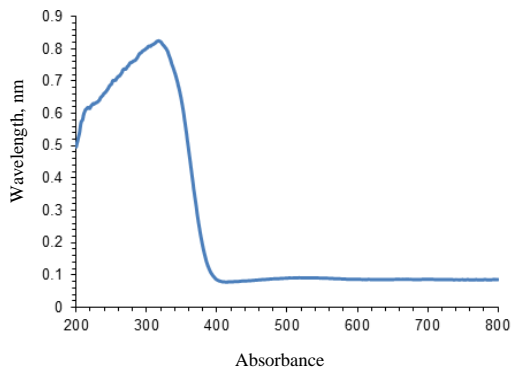
### *UV-Visible spectroscopy analysis*

Figure 2 shows the UV-visible spectra of hydrothermally synthesized TiO<sub>2</sub> powder. This spectra of TiO<sub>2</sub> is the wavelength range of 150-800AU. The maximum absorbance is 0.8 for

wavelength 328AU and band gap is 3.74eV. The  $\text{TiO}_2$  exists in three different crystals modifications, that is as anatase (tetragonal crystal structure with 3.2eV energy gap<sup>13</sup>), rutile (tetragonal crystal structure with 3.2eV energy gap), and brookite (orthorhombic with 2.96eV energy gap). Among the three phases rutile is most stable phase, which can be hydrothermally prepared.



**Figure 1.** SEM image of thick film

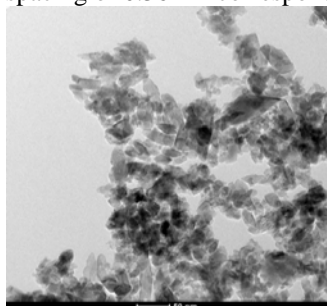


**Figure 2.** UV-visible spectra of synthesized  $\text{TiO}_2$  powder

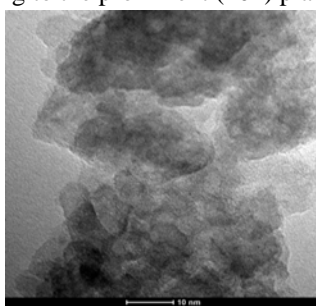
#### TEM and SEAD analysis

Figure 3(a) and (b) shows TEM images of hydrothermally synthesized  $\text{TiO}_2$ . It has been observed that the rice grain shape nanocrystallite  $\text{TiO}_2$  showed an agglomerated status, where magnified image. Figure 3(b) shows atoms are arranged in definite manner and d spacing is 0.36 nm.

Figure 4 shows selected area diffraction pattern, reveals that  $\text{TiO}_2$  is predominantly single crystalline anatase<sup>14</sup>. The lattice-resolved image shown in Figure 4 with lattice spacing of 0.36 nm corresponding to the prominent (101) plane.



(a)



(b)

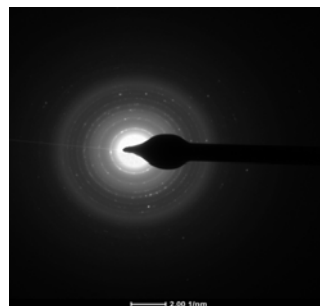


**Figure 4.** SEAD of synthesized  $\text{TiO}_2$  powder

**Figure 3.** TEM images of synthesized  $\text{TiO}_2$  powder

#### X-Ray diffraction analysis

Figure 5 shows the x-ray diffraction pattern of hydrothermally synthesized  $\text{TiO}_2$ . The pattern is well matches with PDF 01-070-2556 data<sup>15</sup>. The sharp peaks indicate that  $\text{TiO}_2$  is well crystalline; the % crystallinity is 93.3%. The average grain size was determined by using Scherer formula and was estimated to be 262 nm.

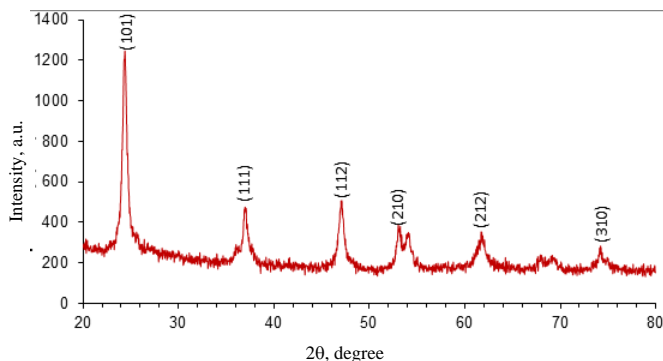


**Figure 5.** X-Ray diffraction pattern of  $\text{TiO}_2$

#### *I-V characteristics of $\text{TiO}_2$ thick films*

Figure 6 Shows the I-V characteristics which represent variation of electric current (pA) versus change in voltage (volt) across the thick film of the  $\text{TiO}_2$  thick film at room temperature. It has been noted from the graph that the contacts fabricated on the film were ohmic in nature.

#### *Electrical conductivity*

Figure 7 represents the variation of conductivity with temperature for pure films. It is clear from the graphs that the conductivity is varying approximately linearly with temperature. Conductivity of the films goes on increasing with an increase in temperature. Hence resistivity goes on decreasing with increase of temperature. Therefore, material exhibit negative temperature coefficient of resistance (NTC).

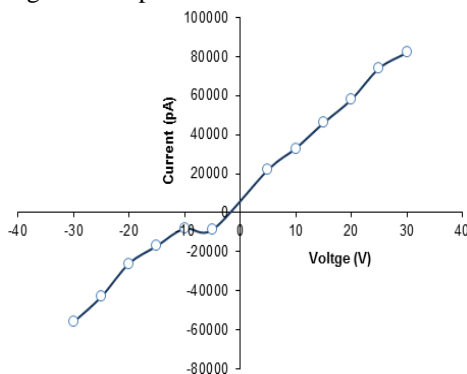


**Figure 6.** Variation of electric current versus applied voltage graph of  $\text{TiO}_2$  thick film

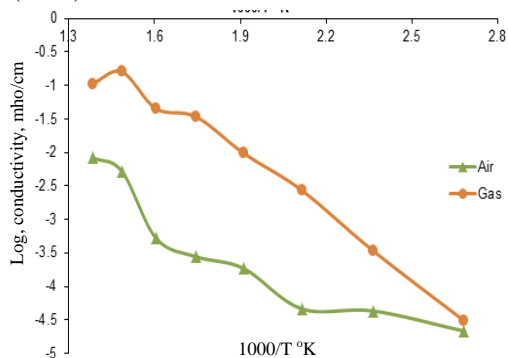


**Figure 7.** Variation of electrical conductivity with temperature

#### *Sensitivity of $\text{TiO}_2$ films*

The gas sensing performance of  $\text{TiO}_2$  thick films were studied by using static measurement system. The conductance of  $\text{TiO}_2$  thick film resistors were measured by means of conventional circuitry by applying constant voltage and measuring the current by Pico ammeter as a function of temperature in air as well as in  $\text{CO}$ ,  $\text{CO}_2$ ,  $\text{H}_2$ ,  $\text{NH}_3$ ,  $\text{Cl}_2$ ,  $\text{H}_2\text{S}$ , LPG, gas atmosphere (800 ppm concentration). The operating temperature was varied at the interval of  $100^\circ\text{C}$  up to  $450^\circ\text{C}$ . From the measured conductance in air as well as in gas atmosphere, the gas response was determined at particular operating temperature using the equation 1.

$$S = \frac{(G_{gas} - G_{air})}{G_{air}} \quad (1)$$

Where  $G_{air}$  = Conductance of sensor in air medium.

$G_{gas}$  = Conductance of sensor in gas medium

Figure 8 shows the variation of sensitivity of TiO<sub>2</sub> films to H<sub>2</sub>S gas (1000 ppm) with operating temperature ranging from 100 to 450 °C. The response goes on increasing with operating temperature, attains its maximum (122) at 300 °C and then decreases with a further increase in operating temperature.

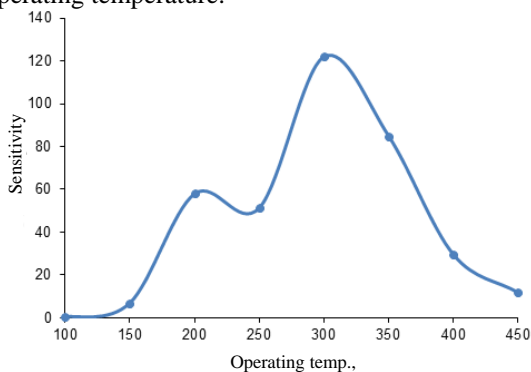


**Figure 8.** Variation of sensitivity of TiO<sub>2</sub> films to H<sub>2</sub>S gas

#### Selectivity of TiO<sub>2</sub> thick films for various gases

Figure 9 shows the histogram of the selectivity of TiO<sub>2</sub> thick film for various gases. The TiO<sub>2</sub> thick films were selective to H<sub>2</sub>S gas against the other tested gases at 300 °C. The sensitivity of thick films were 122 for H<sub>2</sub>S gas.

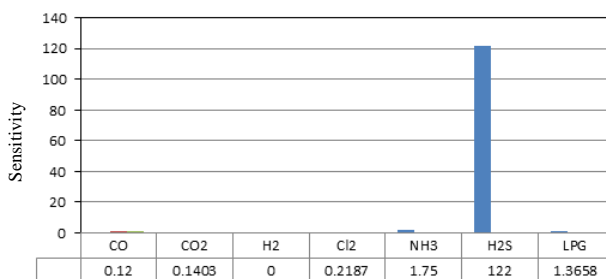


**Figure 9.** Selectivity of TiO<sub>2</sub> thick film

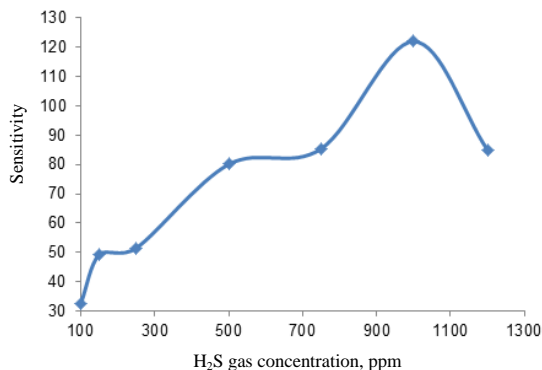
#### Sensitivity of thick film by varying H<sub>2</sub>S gas concentration

Figure 10 shows the sensitivity of TiO<sub>2</sub> thick film by varying H<sub>2</sub>S gas concentration (ppm). The film shows maximum sensitivity for 1000 ppm to H<sub>2</sub>S gas. The sensitivity increases with gas concentration but decreases feature due to saturation.

#### Gas sensing mechanism

The gas sensing mechanism belongs to the surface controlled type which is based on the change of the electrical conductance of the semiconducting material upon exposure to H<sub>2</sub>S gas. The gas sensitivity is a function of grain size, surface state and oxygen adsorption.

The surface area generally provides more adsorption-desorption sites and thus the higher sensitivity. The H<sub>2</sub>S sensing mechanism is based on the change in conductance of TiO<sub>2</sub> thin film, which is controlled by H<sub>2</sub>S species and the amount of chemisorbed oxygen on the surface. It is known that atmospheric oxygen molecules are adsorbed on the surface of semiconductor oxides in the form of O<sup>2-</sup>, O<sup>-</sup> or O<sup>•</sup>.

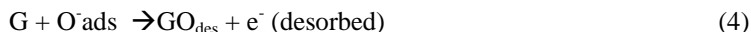


**Figure 10.** Sensitivity of thick films by varying H<sub>2</sub>S gas concentration

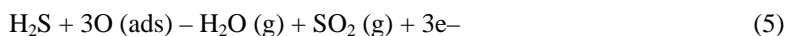
The reaction kinematics may be explained by the following reactions:



On contact with the gas being sensed.



The presence of chemical adsorbed oxygen could cause electron depletion in the thin film surface and building up of Schottky surface barrier; consequently, the electrical conductance of the thin film decreased to a minimum. The TiO<sub>2</sub> thin film interacts with oxygen by transferring the electron from the conduction band to adsorbed oxygen atoms. The response to H<sub>2</sub>S can be explained as a reaction of gas with the O<sub>2</sub> (ads)–.



With this reaction, many electrons could release to thick film surface. This could make the Schottky surface barrier decrease; with the depletion layer thinner; consequently, the electrical conductance of the thick film increases as shown in Figure 11.

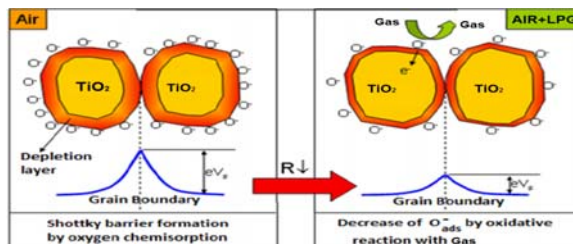


**Figure 11.** Gas sensing mechanism

More gas would be absorbed by the thick film surface; consequently, the gas sensitivity was enhanced. Increase in operating temperature causes oxidation of large number of H<sub>2</sub>S molecules, thus producing very large number of electrons. Therefore, conductivity increases to a large extent.

This is the reason why the gas sensitivity increases with operating temperature. However, the sensitivity decreases at higher operating temperature, as the oxygen adsorbents are desorbed from the surface of the sensor<sup>16</sup>. Also, at higher temperature, the carrier concentration increases due to intrinsic thermal excitation and the Debye length decreases. This may be one of the reasons for decreased gas sensitivity at higher temperature<sup>17</sup>.

## Conclusion

The rice grains-shaped TiO<sub>2</sub> nanostructures were synthesized by using hydrothermal method. Anatase is found to be a predominant phase. Powder XRD shows grain size 174.6 nm and % crystallinity is 93.3%. Increase in band gap represents formation of nanostructure. The thick films are prepared by using screen printing techniques. The thick films are sensitive to H<sub>2</sub>S gas against all other tested gases.

## Acknowledgement

The authors are grateful to Dr. Dilip Dhondge Principal K.T.H.M. College Nasik, Maharashtra, India for providing laboratory facilities. The authors are also thankful to Dr. V. B. Gaikwad, Director, B.C.U.D. Pune University for encourage to do research.

## References

1. Fujishima A, Rao T N and Tryk D A, *J Photochem Photobiol C1*, 2000, 1-21.
2. Gratzel M, *Nature*, 2001, **414**, 338; DOI:10.1038/35104607
3. Zhu Y, Shi J, Zhang Z, Zhang C and Zhang X, *Anal Chem.*, 2002, **74**(1), 120-124; DOI:10.1021/ac010450p
4. Park Y H, Song H K and Lee C S, *J Ind Eng Chem.*, 2008, **14**(6), 818.
5. Kominami H, Muratami S, Katro J, Y Kera Y and Ohtani B, *J Phys Chem.*, 2002, **106**(40), 10501-10507; DOI:10.1021/jp0147224
6. Fujishima A and Honda K, *Nature*, 1972, **238**, 37; DOI:10.1038/238037a0
7. Ganesh Patil E, Kajale D D, Gaikwad V B, Pawar N K and Jain G H, *Sens Transducers Journal*, 2012, **137**(2), 47.
8. Shinde S D, Patil G E, Kajale D D, Gaikwad V B and Jain G H, *Int J Nanoparticles*, 2012, **5**(2), 126-135; DOI:10.1504/IJNP.2012.046239
9. Kajale D D, Patil G E, Gaikwad V B, Shinde S D, Chavan D N, Pawar N K, Shirsath S R and Jain G H, *Int J Smart Sens Intelligent System*, 2012, **5**(2), 382-400
10. Pawar N K, Kajale D D, Patil G E, Wagh V G, Gaikwad V B, Deore M K and Jain G H, *Int J Smart Sens Intelligent System*, 2012, **5**(2), 441-457
11. Shinde S D, Patil G E, Kajale D D, Gaikwad V B and Jain G H, *J Alloys Comp.*, 2012, **528**, 109-114; DOI:10.1016/j.jallcom.2012.03.020
12. Ganesh Patil E, Kajale D D, Ahire P T, Chavan D N, Pawar N K, Shinde S D, Gaikwad V B and Jain G H, *Bull Mater Sci.*, 2011, **34**(1), 1-9; DOI:10.1007/s12034-011-0045-0
13. Agatino Di Paola, Marianna Bellardita and Leonardo Palmisano, *Catalysts*, 2013, **3**, 36-73; DOI:10.3390/catal3010036
14. Peining Z, Nair A S, Shengyuan Y and Ramakrishna S, *Mater Res Bull.*, 2011, **46**(4), 588-595; DOI:10.1016/j.materresbull.2010.12.025
15. Lacks D J and Gordon R G, *Phys Rev B*, 1993, **48**, 2889; DOI:10.1103/PhysRevB.48.2889
16. Windichamann H and Mark P, *J Electrochem Soc.*, 1979, **126**(4), 627-633; DOI:10.1149/1.2129098